



# COMPUTATIONAL STUDY OF LEADING EDGE JET IMPINGEMENT COOLING WITH A CONICAL CONVERGING HOLE FOR BLADE COOLING

Chaina Ram, Seralathan Sivamani, Micha Premkumar T and Hariram V

Department of Mechanical Engineering, Hindustan Institute of Technology and Science, Padur, Tamil Nadu, India

E-Mail: [siva.seralathan@gmail.com](mailto:siva.seralathan@gmail.com)

## ABSTRACT

Leading edge of the gas turbine blades is subjected to highest temperature. Jet impingement cooling is an efficient technique for leading edge blade cooling. In this present study, a single baseline cylindrical hole and the proposed converging conical hole is numerically investigated for convective heat transfer using CFD code, STAR CCM+. The converging angle of the conical hole is 20° and the ratio of diameter is equal to two. The hole diameter is 2.15 cm and the study is carried out at Reynolds number ranging from 11000 to 50000 for a jet impinging length of R/2. The target surface is maintained at constant heat flux of 10000 W/m<sup>2</sup>. Steady-state simulations are performed using Reynolds Averaged Navier Stokes equation along with k- $\omega$ -SST turbulence model for closure. Based on the Nusselt number and temperature distribution, converging conical hole is observed to give a better heat transfer thereby cooling the blades effectively. Around 186 % increase in Nu and 13% decrease in surface temperature of the concave surface is observed at jet impingement point for Re = 23000.

**Keywords:** jet impingement blade cooling, converging conical, cylindrical, reynolds number, nusselt number, CFD.

## NOMENCLATURE

Re	Reynolds number $Re = \left[ \frac{\rho U D}{\mu} \right]$	[--]
d	Hole diameter	[m]
D	Diameter of hole exit	[m]
h	Heat transfer coefficient	[W/m <sup>2</sup> K]
L	Nozzle to wall spacing (impingement length)	[m]
Nu	Local Nusselt number	[--]
T <sub>a</sub>	Ambient temperature	[K]
u	Mean velocity	[m/s]
$\rho$	Air density	[kg/m <sup>3</sup> ]
r	Length along curvature	[m]
$\eta$	Efficiency	[--]
$\beta$	Converging angle	[Rad.]
Pr	Prandtl number	[--]
Q	Heat flux	[W/m <sup>2</sup> ]
$\nu$	Kinematic viscosity	[m <sup>2</sup> /s]
C <sub>p</sub>	Pressure Coefficient	[--]
K	Thermal Conductivity	[W/m K]
R	Stream wise distance from the stagnation point	[m]
$\omega$	Specific turbulence dissipation rate	[s <sup>-1</sup> ]
k	Turbulent kinetic energy	[m <sup>2</sup> /s <sup>2</sup> ]

## INTERODUCTION

The gas turbine engine operates at high temperature for higher efficiency and the efficiency of turbine increases with peak temperature produced in the combustor and temperature sustained by the blades of gas turbine. Leading edge of the gas turbine blades is subjected to highest thermal load and therefore, it requires the efficient cooling. Effusion and jet impingement cooling are the techniques used for cooling the leading edge where the temperature of blade surface is highest. Impingement of high speed jets through tiny holes provide high heat transfer locally. Therefore, it is used in many

engineering applications such as cooling of hot steel plates, tempering of glass, cooling of hot turbine blades and electronic component heat transfer. Among all techniques used for blade cooling, jet impingement has the maximum potential to increase the local heat transfer. However, the construction of impingement hole and flow arrangement reduces the structural strength of the blade and therefore this technique is used in locations where excessively high heat transfer is required. The cooling jet has higher momentum than its surrounding and creates a highly turbulent flow with stagnation zone right under the nozzle exit.

Over the past few decades, numerous numerical and experimental studies were performed to study the flow parameter and heat transfer by jet impingement. Martin [1] studied the heat transfer by convection between the impinging gas jet and solid surface using single and multiple jet systems along with the effect of jet tilting. The variation of local Nusselt number with Reynolds number and effect of jet to wall spacing were discussed by Han and Goldstein [2]. Zuckerman and Lior [3] carried out experimental as well as numerical studies and gave the correlation between Reynolds number and Nusselt number. Florschuetz *et al.* [4] published the effect of cross flow and array of jet on heat Transfer. Lee *et al.* [5] carried out experiments to study the effect of curvature of concave surface on heat transfer parameter by using round impingement jet. Yang *et al.* [6] performed experimental study to analyse the effect of nozzle cross section on cooling of concave surface with flow ejected from holes having different cross sections. The studies showed that heat transfer characteristics differed significantly. Bunker [7] performed experimental study on heat transfer in leading edge without extracting the coolant for other cooling purpose. Han *et al.* [8] studied the effect of impinging jet angle i.e.,  $\pm 45^\circ$  on the target surface and



found that the jet at right angle provides higher Nusselt number compared to other angles.

Haider and Yan [9] numerically analyzed the jet diameter effect on impingement jet cooling at leading edge of the turbine blade. The authors concluded that the Nusselt Number decreased after certain  $L/d$  ratio. Ashok Kumar and Prasad [10] studied the effect of effusion hole in a turbine blade for transpiration cooling along with jet impingement cooling. Effusion holes increased the turbulence which in turn increased the localised heat transfer. Sarfaraz and Ghemai [11] published their numerical work on internal channel cooling via jet impingement using ANSYS Fluent. The sensitivity study of jet impingement cooling on a semi-circular concave surface at constant heat flux with different configurations of jet impingement length and its position at different Reynolds number were also investigated. Investigation on heat transfer enhancement and pressure loss of a double swirl chamber cooling was carried out by Kusterer *et al.* [12]. Several CFD models were analyzed namely, single swirl chamber and double swirl chamber using  $k\omega$ -SST model. Double swirl chamber increased the heat transfer by around 100% compared to impingement without a swirl. Ahmed *et al.* [13] studied different geometry of convergent holes with convergent angle varying from  $5^\circ$  to  $20^\circ$ . Abdulla and Ali [14] studied different configurations of jet impingement length varying from  $R/4$  to  $3R/4$  at different lateral positioning of jet. Recently, studies were also carried out on the effect of hole aspect ratio [15], vortex [16], effusion hole [17], jet spacing [18], aerodynamic behaviour of impingement hole [19] and optimisation of geometry [20].

In this present study, three dimensional steady-state flow parameter and heat transfer characteristics of jet impingement cooling at leading edge of the gas turbine blade is studied using cylindrical hole and converging

conical hole. The convergent angle of the conical hole is kept as  $20^\circ$ . The comparative numerical study is carried out by comparing the converging conical hole with the baseline cylindrical hole configuration.

## NUMERICAL METHODOLOGY

### a) Problem description and computational domain

Leading edge of the gas turbine blade resembles a concave surface and it is considered as hemisphere for the present computational study. The radius of the concave surface is 19.05 cm and the jet impingement hole diameter is 2.13cm. The Reynolds number of the coolant is varied as 11000, 23000 and 50000 [5]. The jet impingement length is kept as  $R/2$  [14]. Length of the hole is kept as  $60d$  for a fully developed flow [12]. Figure-1(a) and 1(b) show the front view and isometric view of the computational domain for jet impingement through a converging conical hole. Convergent angle ( $\beta$ ) for the converging conical hole is kept constant at  $20^\circ$  and the ratio of  $d/D$  is maintained as 2. Similarly, Figures 2(a) and 2(b) show the front view and isometric view of the computational domain for jet impingement through a baseline cylindrical hole configuration. The ratio of  $d/D$  is equal to 1 for cylindrical hole. The configuration details are listed in Table-1. The 3D computational domain is modelled using Solid works.

**Table-1.** Configuration details for cylindrical and conical holes.

Impingement length (L)	Diameter (d)	Reynolds No.
$L = \frac{R}{2}$	$d = 2.15\text{cm}$	Re=11000 Re=23000 Re=50000

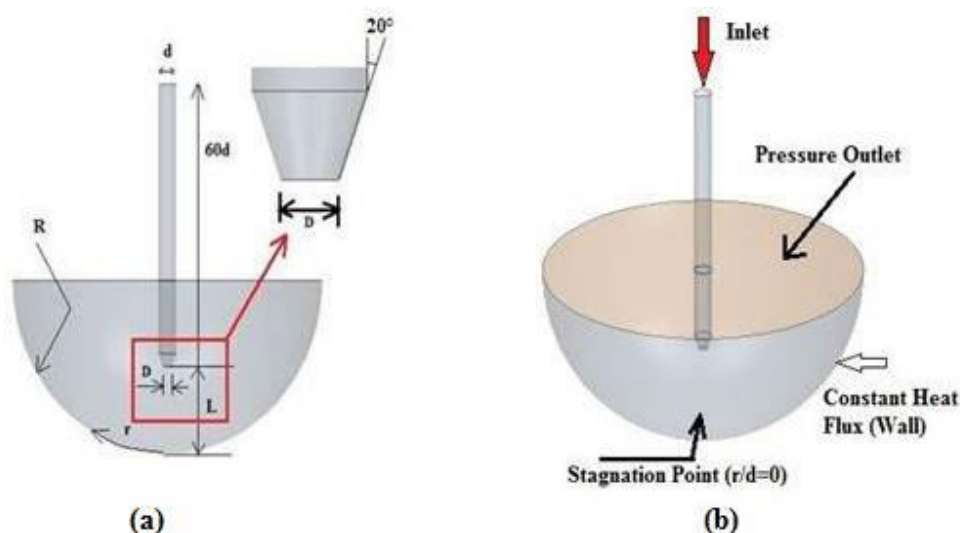


**Figure-1.** (a) Front view of computational model of jet impingement by conical hole  
(b) Isometric view of computational model of jet impingement by conical hole.

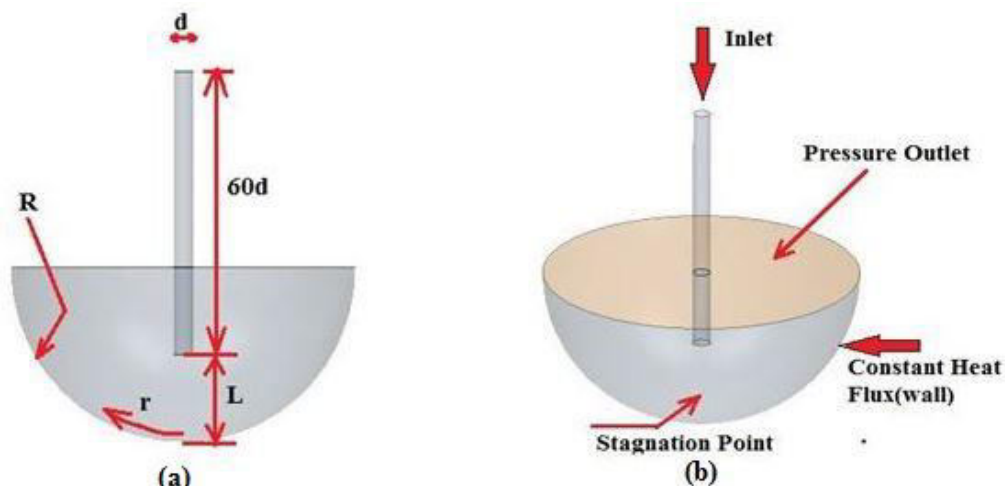


**Figure-2.** (a) Front view of computational model of jet impingement by cylindrical hole  
(b) Isometric view of computational model of jet impingement by cylindrical hole.

### b) Mesh generation

Complete unstructured polyhedral mesh is generated using STAR CCM+. Dense mesh is given at the coolant-jet mixing zone and constant heat wall region. Prism layers are used near the wall (i.e., target surface) and pipe wall. Nearly ten prism layers are introduced to capture the near wall boundary layer viscous effects. Further, a more dense mesh is created in the converging conical hole region to capture the effects in the convergent hole region. Figure 3 and 4 shows the section plane of the meshed fluid domain of a converging conical hole and cylindrical hole configurations.

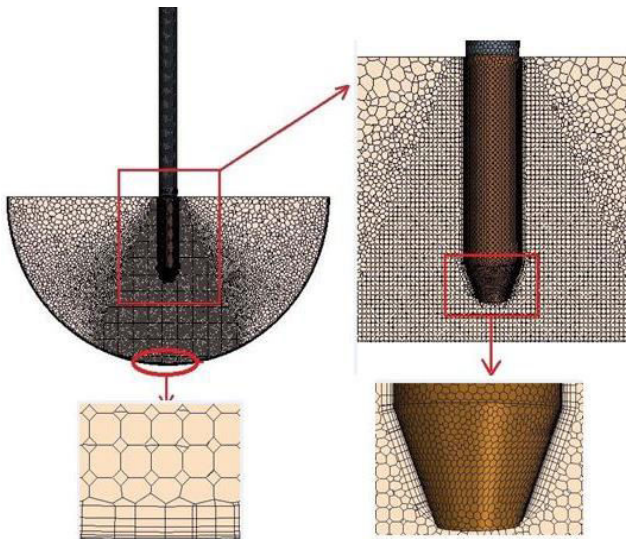


**Figure-3.** Mesh generation of the computational domain with conical hole.

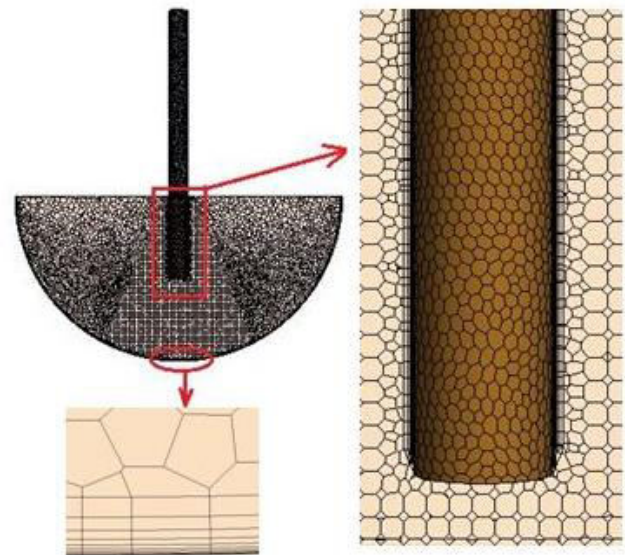


**Figure-4.** Mesh generation of the computational domain with cylindrical hole.

### c) Validation, grid independent study and turbulence model study

CFD code STAR CCM+ which solves the continuity, momentum and energy equations is used for this present numerical investigation. Experimental results observed by Lee *et al.* [5] for local Nusselt number along the curvature for  $L/d=4$ ,  $Re = 23000$  and hole diameter 2.15cm is validated and shown in Figure-5. Three different turbulence models namely, V2f,  $k\epsilon$  and  $k\omega$ -SST turbulence model are used for capturing the flow physics. As can be seen in Figure-5,  $k\omega$ -SST turbulence model gives a closer result with the experimental result [5]. Hence,  $k\omega$ -SST turbulence model is used for further numerical analysis of all the cases in this present study. Figure-6 shows the variation of Nusselt number at stagnation point (i.e.,  $r/d$  equal to zero) with different mesh count. The variation of stagnation Nusselt number is also tabulated in Table-2. As the relative error in Nusselt



number is almost negligible beyond the grid count of 1.45 millions, this mesh is taken as a reference mesh count for all the configurations.

**Table-2.** Grid independence study.

Grid	Number of element	Nusselt number (Nu)	Relative error of Nu in %
1	796504	172.2188	29.91%
2	1039418	143.0705	7.92%
3	1203600	135.25	2.02%
4	1450000 [Reference]	132.565	0%
5	1610000	132.4731	0.069%
6	1790000	132.52	0.033

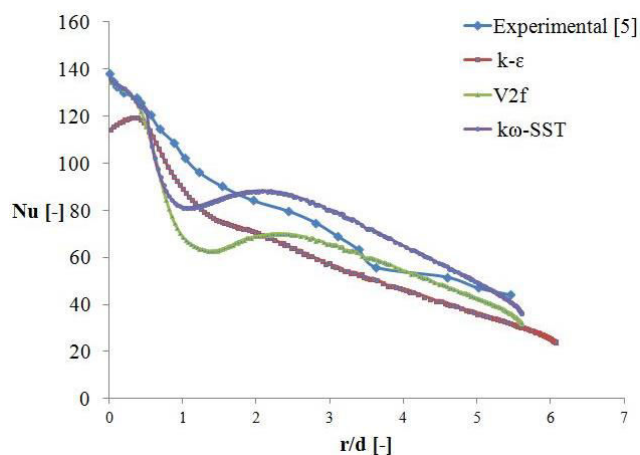


**Figure-5.** Validation of stream wise distributions of local Nusselt number.

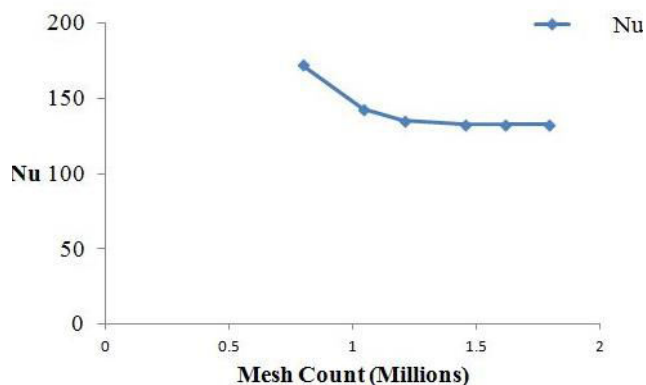


**Figure-6.** Grid independency study.

#### d) Boundary conditions

The whole domain is considered as fluid domain. Inlet boundary condition is defined as mass flow through which the coolant air enters at a mass flow rate of  $1.14 \times 10^{-3}$  kg/s and the temperature of the coolant air is specified as 300K. Outlet boundary condition is considered as pressure outlet and it is kept constant at a atmospheric pressure of 101325 Pa. The wall of the concave surface is defined as wall with no-slip condition and it is maintained at a constant heat flux of  $10000 \text{ W/m}^2$ . Interface is introduced

between the concave surface and side wall of pipe and the interface type is baffle interface. Interface between the concave region and exit of the pipe is also introduced. Wall of the pipe is defined as adiabatic wall. SIMPLE algorithm is invoked and second order upwind scheme is used for numerical solutions.  $k\omega$ -SST turbulence model is used to achieve the closure and all the governing equations are solved under steady-state conditions. The normalized convergence criteria for is kept as  $10^{-6}$  for continuity equation and  $10^{-4}$  for the momentum and energy equations. Table-3 shows the boundary conditions enforced in this present study.

**Table-3.** Boundary conditions [5, 12].

Boundary location	Boundary condition	Values
Inlet	Mass flow rate	$1.14 \times 10^{-3} \text{ Kg/s}$
Outlet	Pressure	101325 pa
Wall	No slip; Stationary wall	-
Inlet	Temperature	300K
Wall	Constant heat Flux	$10000 \text{ W/m}^2$

#### RESULT AND DISCUSSIONS

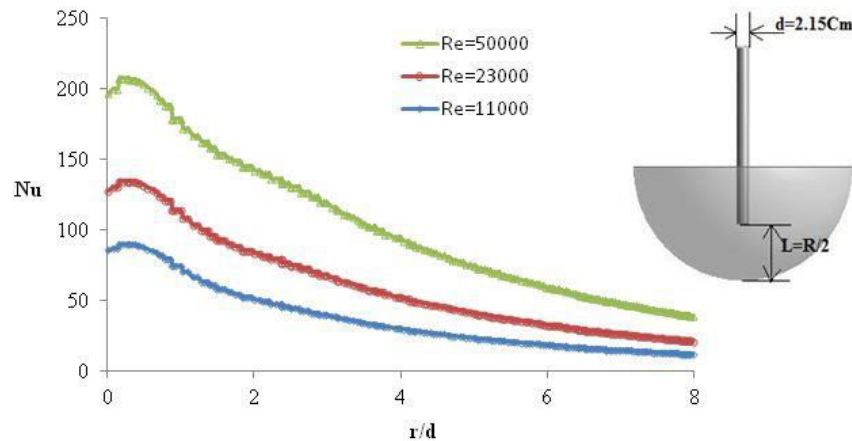
Distribution of local Nusselt number stream wise along the concave surface for the impinging jet through a cylindrical hole of diameter 2.15cm and jet impingement length of R/2 at Reynolds number 11000, 23000 and 50000 is shown in Figure-7. Figure-8 shows the distribution of local Nusselt number stream wise along the concave surface for the impinging jet through a converging conical hole. As can be seen in Figure-8, first peak value of Nusselt number is observed at the point of jet impingement on the concave surface and the second peak value of Nusselt number is realized which is due to circulation effect. This results in increased turbulence and enhances the heat transfer. Similar trend is also observed for cylindrical hole configuration as seen in Figure-7. In general, the Nusselt number increases with increase in Reynolds number. This is due to increase in velocity of the potential core region of jet which reduces the boundary



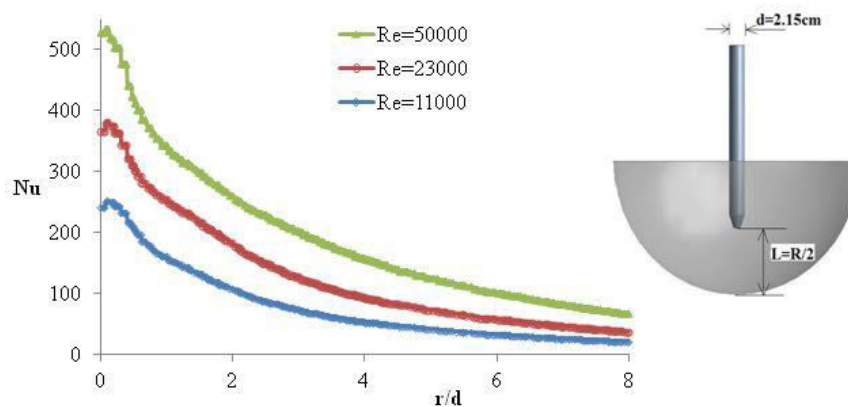


layer thickness formation at stagnation region thereby enhancing the heat transfer. At  $Re = 23000$ , Nusselt number increased by 186 % for jet impingement through

converging conical hole in comparison with cylindrical hole. Similarly, it increased by 185% and 170.5% for  $Re = 11000$  and 50000 respectively.

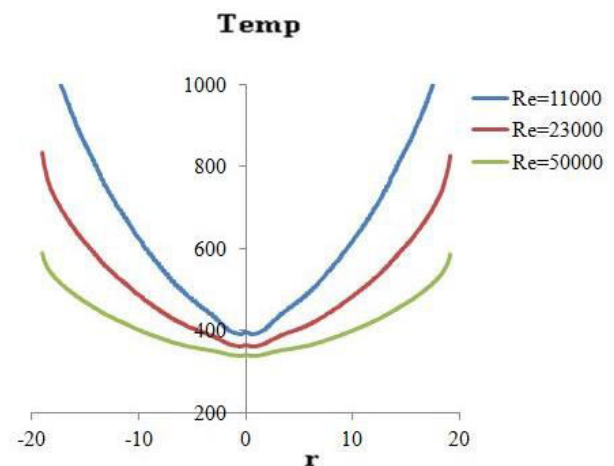


**Figure-7.** Distribution of local Nu stream wise along the concave surface for the impinging jet through a cylindrical hole.

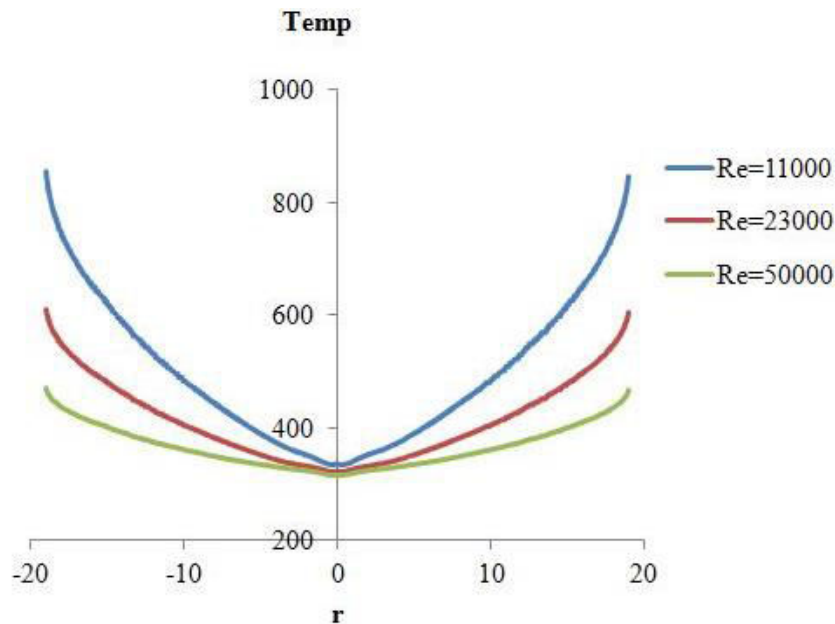


**Figure-8.** Distribution of local Nu stream wise along the concave surface for the impinging jet through a converging conical hole.

Wall temperature distribution along the curvature of the target surface for cylindrical hole and converging conical hole is shown in Figure-9 Figure-10 respectively. Lowest temperature is attained at the point of jet impingement and the temperature increases gradually along the stream wise position in the concave surface. On comparing the cylindrical and converging conical hole configurations, 15.58% decrease in temperature is observed at jet impingement point for  $Re = 11000$ . Similarly, 13% and 7.68 % decrease in temperature is realized for at  $Re = 23000$  and 50000 respectively.



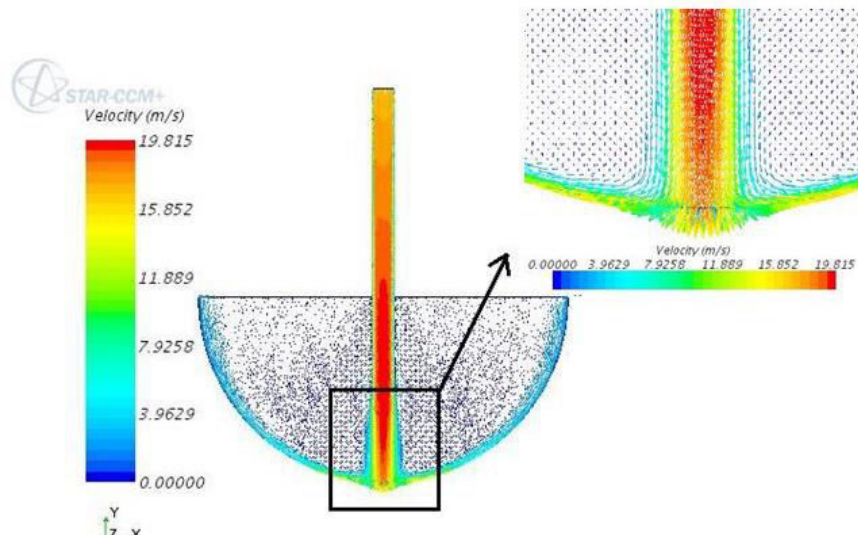
**Figure-9.** Temperature along concave curvature for impingement through cylindrical hole.



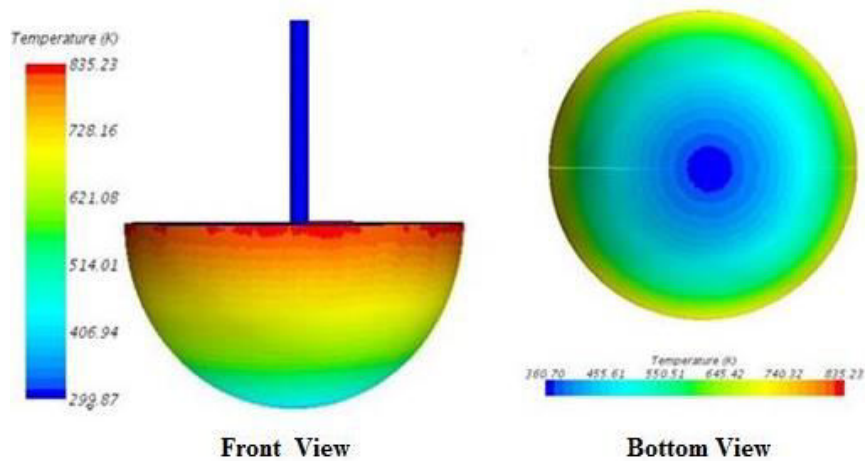
**Figure-10.** Temperature along concave curvature for impingement through converging conical hole.

In general, the minimum temperature reduces with increase in Reynolds number for both the configurations. Two minimum temperature points are observed on the concave surface, one at the jet impinging point and another just away from the stagnation region, this effect is due to the circulation. Figure 11 and 12 show the velocity vector plot and temperature distribution of jet

impingement through a cylindrical hole at  $Re = 23000$ . Highest velocity of the impinging jet reaches 19.81 m/s in the potential core region of the jet and the highest wall temperature is 835.23 K for constant heat flux of 10000 W/m<sup>2</sup>. Along the target surface, it is cooled to 366.66 K at the jet impingement point.



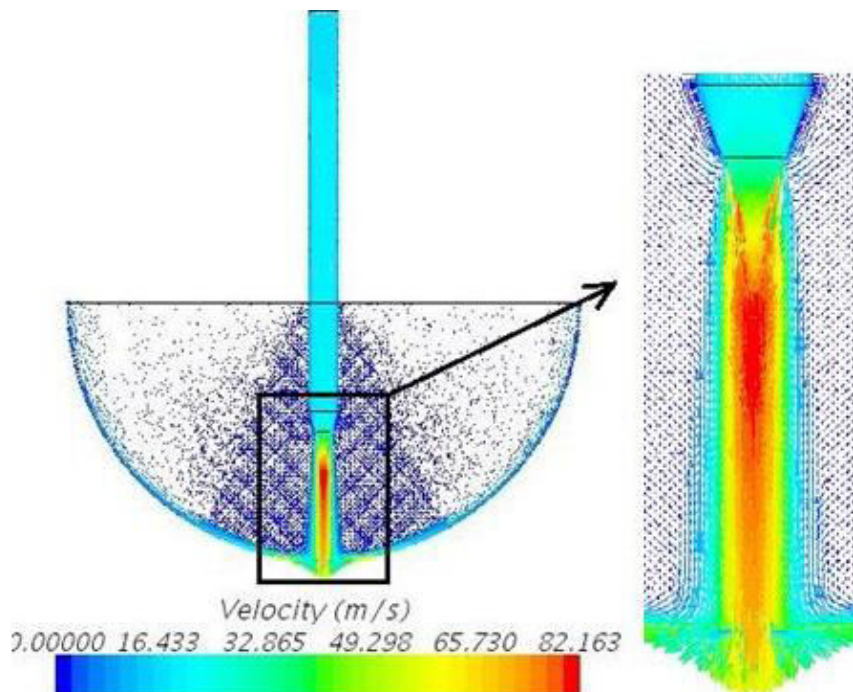
**Figure-11.** Velocity vector for jet impingement through cylindrical hole.



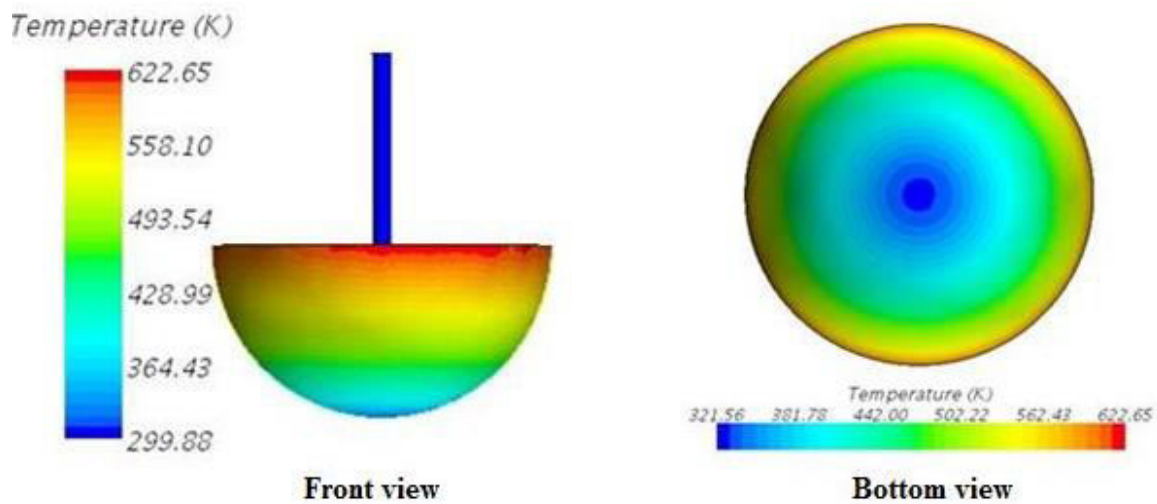
**Figure-12.** Contour of temperature distribution for impingement through cylindrical hole.

Figure-13 shows the global velocity distribution for jet impingent cooling using converging conical configuration at  $Re = 23000$ . Highest velocity reaches 82.163 m/s in the potential core region which reduces the boundary layer thickness formation at the point of jet impingement thereby leading to a higher Nusselt number compared to impingement through a cylindrical hole.

Figure-14 shows the local temperature distribution for the above case. The minimum temperature is found at the stagnation point on hemispherical surface, which then it increases away from the stagnation point. Highest wall temperature is found to be 622.65 K for constant heat flux of  $10000 \text{ W/m}^2$  and the target surface at the point of jet impingement is cooled to 299.88 K.



**Figure-13.** Velocity vector for jet impingement through converging conical hole.



**Figure-14.** Temperature distributions for jet impingement through converging conical hole.

Figure 15, 17 and 19 shows the comparison of Nusselt Number between baseline cylindrical hole and converging conical hole at  $Re = 11000$ ,  $23000$  and  $50000$  respectively. Similarly, Figure 16, 18 and 20 shows the comparative temperature distribution between these two configurations at different Reynolds number. In general, converging conical hole configuration gives a better cooling performance at leading edge cooling of the gas turbine blade cooling. Highest increase in Nusselt number by 186% is obtained for  $Re = 23000$  and highest  $Nu$  value is obtained for  $Re = 50000$ . Maximum percentage drop in temperature is obtained for  $Re = 23000$  and a minimum temperature of  $299.88\text{ K}$  is obtained for  $Re = 23000$ .

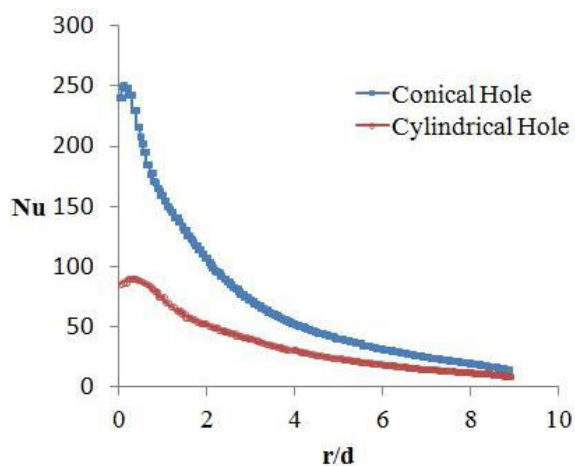


**Figure-15.** Comparison of  $Nu$  for cylindrical and converging conical hole at  $Re\ 11000$ .

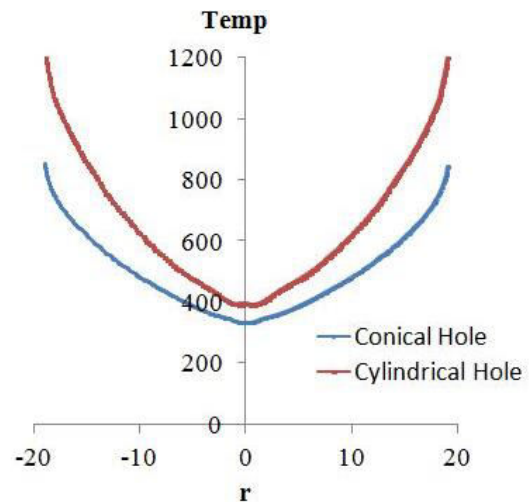


**Figure-16.** Comparison temperature distribution for cylindrical and converging conical hole at  $Re\ 11000$ .

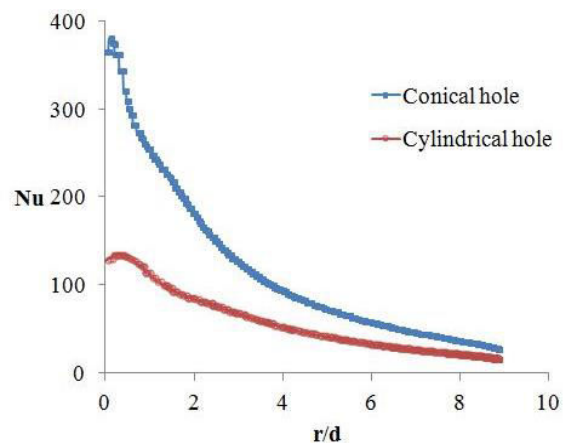


**Figure-17.** Comparison of  $Nu$  for cylindrical and converging conical hole at  $Re\ 23000$ .



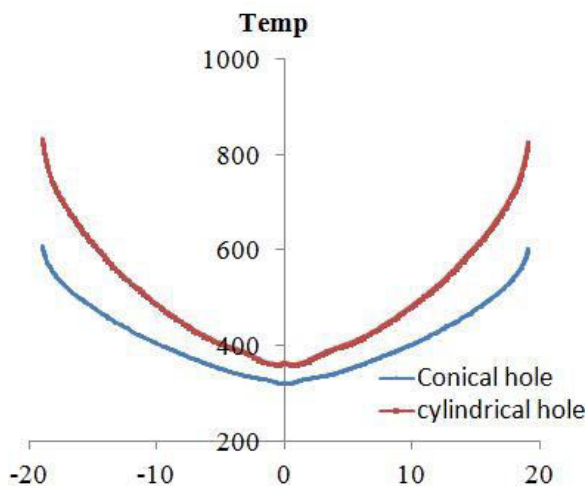


**Figure-18.** Comparison temperature distribution for cylindrical and converging conical hole at Re 23000.

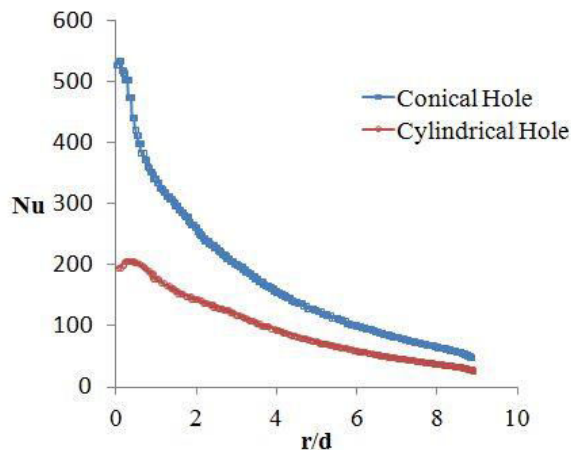


**Figure-19.** Comparison of Nu for cylindrical and converging conical hole at Re 50000.

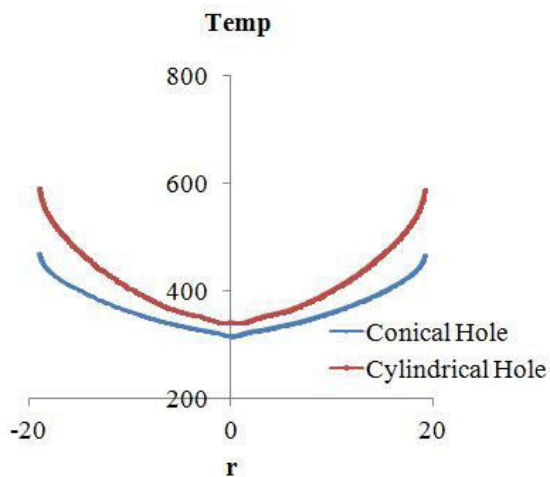


**Figure-20.** Comparison temperature distributions for cylindrical and converging conical hole at Re 50000.

## CONCLUSIONS

Based on the comparative numerical study of single impinging jet through cylindrical and converging conical hole on concave surface, the key observations are given below:

- Nusselt number increase varied by 170 to 186% for Reynolds number ranging from 11000 to 50000 in converging conical configuration.
- Temperature on the jet impinging point decreased by 7.68 % to 15.58% as the jet is impinged through converging conical hole for Re 11000 to 50000.
- Increase in Reynolds number increased the Nusselt number at jet impinging point as well as along the curvature.
- Increase in Nusselt number results in increase in heat transfer thereby leading to enhanced blade cooling at leading edge.

The results from this comparative studies shows that converging conical hole at Re = 23000 gives a better leading edge blade cooling.

## REFERENCES

- [1] Martin H. 1977. Heat and mass transfer between impinging gas jets and solid surfaces. *Adv. Heat Transfer*. 13: 1-60.
- [2] Han B and Goldstein. 2001. Jet-Impingement heat transfer in gas turbine system, *Annals of the New York Academy of Science*. 10: 47-191.
- [3] Zuckerman and Noam Lior. 2005. Impingement Heat Transfer: Correlations and Numerical Modelling, *J. Heat Transfer*. 127(5): 544-552(9 pages).
- [4] Florschuetz L. W., Metzger D. E., and Su C. C. 1984. Heat transfer characteristics for jet array impingement with initial cross flow, *J. Heat Transfer*. 106: 34-41.
- [5] Lee D. H., Chung Y.S. and Won S.Y. 1999. The effect of concave surface on heat transfer from a fully developed round impinging jet. *International journal of Heat and Mass Transfer*. 42: 2489-2497.
- [6] Geunyoung Yang, Mansoo Choi, Joon Sik Lee. 1999. An experimental study of slot jet impingement cooling on concave surface: effects of nozzle configuration and curvature. *International Journal of Heat and Mass Transfer*. 42: 2199-2209.



- [7] Bunker R.S. 2013, Gas Turbine Cooling: Moving from Macro to Micro Cooling. Proceeding of ASME Turbo Expo, GT2013-94277.
- [8] Han J.-C., Dutta S. and Ekkad S. 2000. *Gas Turbine Heat Transfer and Cooling Technology*, Taylor and Francis, New York. 13: 357.
- [9] Syed A. Haider and Terry X. Yan, 2016. Jet Diameter Effect on Impingement Jet Cooling on The Leading Edge of A Turbine Blade. 54<sup>th</sup> AIAA Aerospace Sciences Meeting, San Diego, California, USA. 12: 0905.
- [10] M. Ashok Kumar and Bhamidi V.S.S.S. Prasad. 2012. International Journal of Fluid Machinery and Systems. 5: 2, ISSN (Online): 1882-9554.
- [11] Janajreh I. Sarfraz O. and Ghenai C. 2014. Numerical simulation of internal channel cooling via jet impingement in fluent and its sensitivity study. HEFAT 2014 10<sup>th</sup> International Conference on Heat Transfer, Fluid Mechanics and Thermodynamics, 14-16 July 2014, Orlando, Florida, USA.
- [12] Karsten Kusterer, Gang Lin, Dieter Bohn, Takao Sugimoto, Ryozi Tanaka, Masahide Kazari. 2014. Leading Edge Cooling of a Gas Turbine Blade with Double Swirl Chambers. GT2014-25851, V05AT12A024:11
- [13] F. Ben Ahmed, R. Tücholtke, B. Weigand and K. Meier. 2011. Numerical investigation of heat transfer and pressure drop characteristics for different hole geometries of a turbine casing impingement cooling system. Proceedings of ASME Turbo Expo 2011.
- [14] Abdulla R. Al Ali. 2015. Numerical Simulation of Turbine Blade Cooling via Jet Impingement. The 7<sup>th</sup> International Conference on Applied Energy - ICAE2015, Energy Procedia. 75: 3220-3229.
- [15] Zhao Liu, Jun Li, Zhenping Feng, Terrence Simon. 2015. Numerical study on the effect of jet nozzle aspect ratio and jet angle on swirl cooling in a model of a turbine blade leading edge cooling passage. International Journal of Heat and Mass Transfer. 90: 986-1000.
- [16] Dushyant Singh, B. Premachandran, Sangeeta Kohli. 2017. Double circular air jet impingement cooling of a heated circular cylinder. International Journal of Heat and Mass Transfer. 109: 619-646.
- [17] Tan Xiao-ming, Zhang Jing-zhou, Xu Hua-sheng. 2015. Experimental investigation on impingement/effusion cooling with short normal injection holes. International Communications in Heat and Mass Transfer. 69: 1-10.
- [18] Arash Azimi, Mehdi Ashjaee, Pooyan Razi. 2015. Slot Jet Impingement Cooling of a Concave Surface in an Annulus, Experimental Thermal and Fluid Science. 68: 300-309.
- [19] Changhe Du, Liang Li, Xiaojun Fan, Zhenping Feng. 2017. Rotational influences on aerodynamic and heat transfer behaviour of gas turbine blade vortex cooling with bleed holes, Applied Thermal Engineering (Article in Press).
- [20] Zhongran Chi, Haiqing Liu, Shusheng Zang. 2017. Geometrical optimization of non uniform impingement cooling structure with variable-diameter jet holes, International Journal of Heat and Mass Transfer. 108: 549-560.